

Interaction of 0.5- and 1.0-Mev Neutrons with Some Heavy Elements*

R. C. ALLEN, R. B. WALTON,† R. B. PERKINS,† R. A. OLSON, AND R. F. TASCHEK
Los Alamos Scientific Laboratory, University of California, Los Alamos, New Mexico

(Received July 26, 1956)

The angular distributions of 0.5-Mev neutrons elastically scattered by Au, Bi, U^{238} , U^{235} , and Pu^{239} and of 1.0-Mev neutrons elastically scattered by the latter three materials have been measured. The differential and total elastic scattering cross sections, the elastic transport cross sections, and the inelastic collision cross sections are presented. Some theoretical angular distributions and cross sections based on a complex square-well model for U^{238} are also included. The angular distributions of fission neutrons produced by 0.5- and 1.0-Mev incident neutrons are found to be isotropic, and the ratio of $\bar{p}(Pu^{239})$ to $\bar{p}(U^{235})$ is 1.3 ± 0.2 at both energies.

I. INTRODUCTION

THE angular distributions of elastically scattered neutrons have been studied by several authors. A summary of the general features of these results as a function of atomic weight and energy has recently been made.¹ Very few data, however, have been reported on the fissionable elements. The increasing detail involved in calculations pertaining to chain-reacting systems has made it desirable to obtain more information about relevant cross sections. The scattering of neutrons with energies less than 1 Mev is particularly important. From the theoretical point of view, considerable interest has been shown lately in the optical model^{2,3} of the nucleus. The total cross sections averaged over resonances in the 1- to 3-Mev region and the angular dependence of neutron elastic scattering at 1 Mev have been reasonably well reproduced by describing the interaction in terms of a complex square-well potential of the form

$$V = -V_0(1 \pm i\zeta), \quad r < R$$

$$V = 0, \quad r > R$$

where the potential depth V_0 and the absorption parameter ζ are constants and R is the nuclear radius.

The present work was undertaken to provide more heavy-element cross sections important to both reactor design and nuclear theory. The differential cross sections for elastically scattered 0.5-Mev neutrons were measured for Au, Bi, U^{238} , U^{235} , and Pu^{239} , and for 1.0-Mev neutrons for the latter three materials. The angular distributions of fission neutrons were also obtained at both energies for U^{235} and Pu^{239} .

II. EXPERIMENTAL ARRANGEMENT

The experimental arrangement is shown in Fig. 1. Neutrons from the $T(p,n)He^3$ reaction were scattered by the sample and detected by a hydrogen recoil counter located in an oil-filled collimator and shield. The counter, a cylinder six inches long with a 1.5-inch inner diameter, was filled with 375 psi of hydrogen. It was located 25 inches from the scattering sample inside the collimator and shield tank. The whole assembly was rotatable about the sample. The minimum angle used was 25° . Scattering of source neutrons into the counter by the front part of the collimator on the side away from the target prevented the use of smaller angles. The highest angle obtainable was 130° , this limit being reached when the shield hit the target tube. The effectiveness of the shield was quite good; the ratio of scattered neutrons to background neutrons was about 2 to 1 at 25° , and 4 to 1 at 130° . The angular resolution of this arrangement was $\pm 3^\circ$. Samples were limited in size by the collimating geometry to $\frac{3}{4}$ -inch diameter spheres. The samples were placed three inches from the $T(p,n)He^3$ neutron source, which was a gas target 2 cm long and with a 0.2-mil aluminum entrance foil. At 0.5 Mev, the neutron energy spread was 60 kev and at 1.0 Mev the spread was 50 kev. For the elements used, these energy spreads were sufficient to average over resonances. The effect of the shield tank on the neutron spectrum at the sample was found to be negligible for neutrons in the energy range detected by the recoil counter.

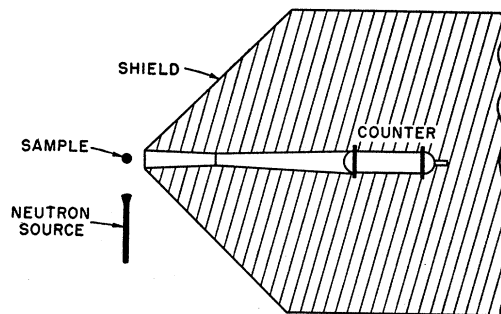


FIG. 1. The experimental arrangement.

* This work performed under the auspices of the U. S. Atomic Energy Commission.

† Summer student from the University of Wisconsin, Madison, Wisconsin.

¹ M. Walt, *Proceedings of the International Conference on the Peaceful Uses of Atomic Energy, Geneva, 1955* (United Nations, New York, 1956), Vol. 2, Paper 588. Dr. Walt's report also includes the preliminary values from this experiment.

² Feshbach, Porter, and Weisskopf, *Phys. Rev.* **96**, 448 (1954).

³ V. F. Weisskopf, *Proceedings of the International Conference on Peaceful Uses of Atomic Energy, Geneva, 1955* (United Nations, New York, 1956), Vol. 2, Paper 830.

III. EXPERIMENTAL PROCEDURE

Since a recoil counter is an energy-discriminating detector, it was possible to reduce the sensitivity of the counter to inelastically scattered neutrons. The biases on the scalers used to record the counter pulses were adjusted in such a manner that only the pulses corresponding to maximum or nearly maximum energy proton recoils were accepted. Two scalers were used at all times. One of these was biased such that the detection efficiency relative to the primary energy was reduced to 0.6 for neutrons having 90% of the primary energy and to 0.2 for neutrons having 80% of the primary energy. When data were taken with 0.5-Mev neutrons, the second scaler was biased lower, so that the relative efficiencies were 0.9 for 90% of the primary energy, 0.7 for 80%, and 0.3 for 60% of the primary energy. At 1.0 Mev the second scaler bias resulted in efficiencies of 0.8 for 90% and 0.4 for 80% of the incident energy. These efficiencies were obtained as a function of neutron energy by comparing the counts per unit charge on the target from the recoil counter with the counts per unit charge on the target from an energy-insensitive long counter.⁴

Data were taken with the detector at 25°, 130°, and at 15° intervals from 30° to 120° with and without the sample in place. Interspersed were runs made at 0°, without the scattering sample, for measuring the incident flux. By measuring the incident flux in this manner, knowledge of the absolute sensitivity and solid

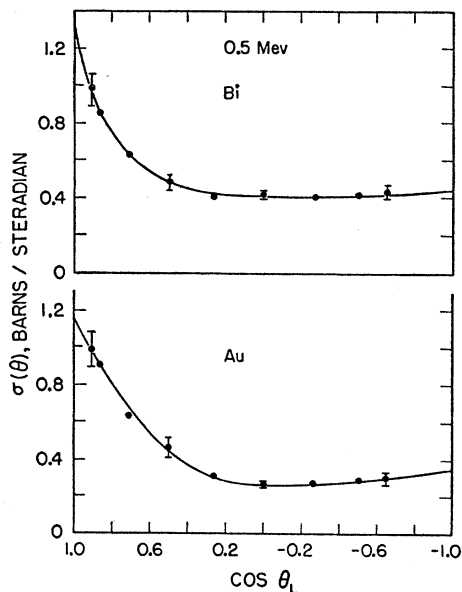


FIG. 2. The differential cross section in barns per steradian for elastic scattering of 0.5-Mev neutrons by Au and Bi plotted as a function of the cosine of the laboratory angle. The errors shown are the standard deviations and the points without errors indicated have errors equal approximately to those of the adjacent points.

⁴ A. O. Hanson and J. L. McKibben, Phys. Rev. **72**, 673 (1947).

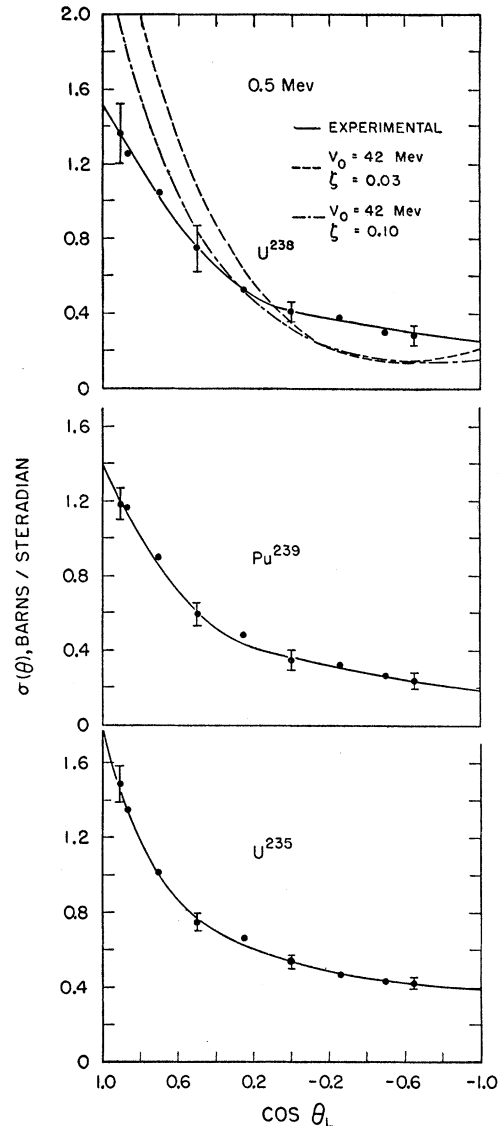


FIG. 3. The differential cross section in barns per steradian for elastic scattering of 0.5-Mev neutrons by U^{238} , U^{235} , and Pu^{239} plotted as a function of the cosine of the laboratory angle. The errors shown are the standard deviations and the points without errors indicated have errors equal approximately to those of the adjacent points. Also shown are the theoretical angular distributions predicted by a complex square-well model using $V_0 = 42$ Mev, $R = 1.45 \times 10^{-13} A^{1/3}$ cm, and $\zeta = 0.03$ and 0.01 .

angle of the counter was not necessary. The cross section was obtained from these data by using

$$\sigma(\theta) = \frac{S(\theta)}{C(0^\circ)} \cdot \frac{1}{FEN} \cdot \frac{d^2 r_1^2}{r_2^2},$$

where $S(\theta)$ is the number of counts at θ due to elastically scattered primaries; $C(0^\circ)$ is the number of counts at 0° due to incident neutrons; F is a factor computed from the total cross section to allow for the flux attenua-

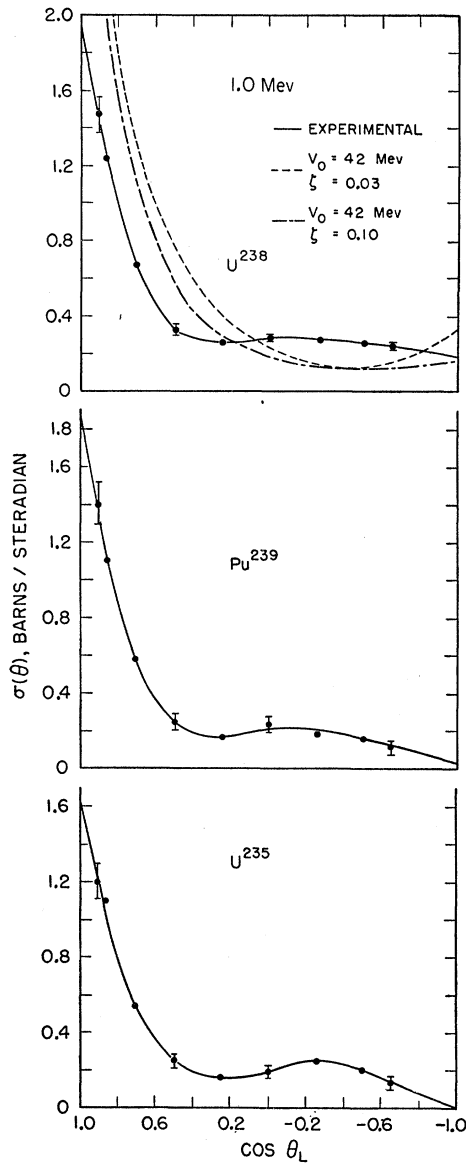


FIG. 4. The differential cross section in barns per steradian for elastic scattering of 1.0-Mev neutrons by U^{238} , U^{235} , and Pu^{239} plotted as a function of the cosine of the laboratory angle. The errors shown are the standard deviations and the points without errors indicated have errors equal approximately to those of the adjacent points. Also shown are the theoretical angular distributions predicted by a complex square-well model using $V_0=42$ Mev, $R=1.45 \times 10^{-13} A^{1/3}$ cm, and $\zeta=0.03$ and 0.10.

tion in the sample; E is the efficiency of the counter for neutrons scattered at angle θ relative to the zero degree efficiency (for heavy elements this is a very small correction); N is the total number of scattering nuclei; d , r_1 , and r_2 are, respectively, the geometric mean distances between the neutron source and the sample, the sample and the counter, and the neutron source and the counter.

For the nonfissionable nuclides, $S(\theta)$ was the differ-

ence between the two runs taken at θ with and without the scattering sample. With the fissionable materials a further complication arose from the fission neutrons, some of which had energies greater than the detector threshold and thus were counted. An experimental correction was made for these neutrons in the following manner. A third scaler was biased to record only pulses corresponding to energies greater than the primary energy. The energy of the primary neutrons was set at 80 kev, which was below the energy to produce counts, and the relative counts in the scalers due only to fission neutrons were observed. This distribution of counts was then normalized to the record of the third scaler for runs using fast primary neutrons. The fission neutron effect was then subtracted.

All runs were normalized by neutron monitoring with a long counter. The effect of scattering by the shield tank into the long counter was measured under conditions of steady beam current and target gas pressure.

IV. RESULTS

After the cross sections were computed with the above formula, the angular distributions were corrected for multiple scattering in the sample by the method developed and tested by Walt and Barschall.⁵ The problem was coded for and solved on an IBM 701 computer. The magnitude of the correction varied from about 15% at 25° to 10% at 45° and from 0 to 5% between 60° and 130° . The final corrected angular distributions based on the high-bias data are given in Figs. 2 through 4. The errors shown are the estimated standard deviations. At the large angles the errors are mostly statistical, whereas at the small angles the statistical errors, multiple scattering errors, and other errors combined are roughly the same.

Table I summarizes the experimental values of the cross sections. The total and fission cross sections were obtained from BNL-325.⁶ The elastic scattering,

TABLE I. Experimental values of elastic scattering, elastic transport, inelastic collision, inelastic collision minus fission, and total cross sections.

Element	Neutron energy (Mev)	σ_t^a (barns)	σ_{el} (barns)	$\sigma_{el tr}$ (barns)	σ_{in} (barns)	$\sigma_{in} - \sigma_t^a$ (barns)
Au	0.5	6.3	5.4	4.0	0.9	
Bi	0.5	6.3	6.3	5.4	0.0	
Pu^{239}	0.5	8.5	6.1	4.1	2.4	0.7
	1.0	7.2	4.1	2.2	3.1	1.3
U^{235}	0.5	7.7	5.9	3.9	1.8	0.6
	1.0	6.7	4.0	2.2	2.7	1.4
U^{238}	0.5	8.2	7.3	4.7	0.9	
	1.0	6.9	5.4	3.5	1.5	

^a The total and fission cross sections were obtained from BNL-325.⁶

⁵ M. Walt and H. H. Barschall, Phys. Rev. **93**, 1062 (1954).

⁶ D. J. Hughes and J. A. Harvey, *Neutron Cross Sections*, Brookhaven National Laboratory Report BNL-325 (Superintendent of Documents, U. S. Government Printing Office, Washington, D. C., 1955).

TABLE II. Theoretical values of total, elastic scattering, elastic transport, and compound nucleus formation cross sections for U^{238} . Parameters are $V_0=42$ Mev, $R=1.45 \times 10^{-13} A^{1/3}$ cm, and $\zeta=0.03$ and 0.10.

Ele- ment	Neutron energy (Mev)	$\zeta=0.03$		$\zeta=0.10$		$\zeta=0.03$		$\zeta=0.10$	
		σ_t (barns)	σ_{el} (barns)	$\sigma_{el\ tr}$ (barns)	σ_c (barns)	σ_t (barns)	σ_{el} (barns)	$\sigma_{el\ tr}$ (barns)	σ_c (barns)
U^{238}	0.5	10.5	9.4	9.1	7.4	4.4	3.7	1.4	2.0
	1.0	8.9	8.4	7.8	6.4	3.7	2.9	1.1	2.0

elastic transport, and inelastic collision cross sections were computed from the data according to the definitions:

$$\sigma_{el} = \int \sigma(\theta) d\omega,$$

$$\sigma_{el\ tr} = \int \sigma(\theta) (1 - \cos\theta) d\omega,$$

$$\sigma_{in} = \sigma_t - \sigma_{el},$$

where $\sigma(\theta)$ is the differential elastic scattering cross section and $d\omega$ is the solid angle. The 1.0-Mev U^{238} angular distribution agrees very well with that previously reported by Walt.¹ The errors in the inelastic collision cross sections are determined primarily from the errors in the total elastic scattering cross sections. Since these latter are 10 to 15%, the errors in the inelastic collision cross sections are about 0.6 to 0.8 b. All the elements studied here except Bi have low-lying levels in the 50-kev region to which inelastic scattering can occur without much loss of energy by the incident neutron. Since the detector did not discriminate effectively against such inelastically scattered neutrons, the inelastic collision cross sections quoted are only lower limits and do not include the effects of low-lying levels. The lowest level in Bi is at 0.9 Mev, and thus for 0.5-Mev primary neutrons there cannot be any inelastic scattering.

The purpose in using the different scaler biases was to get more information on inelastic scattering. The difference between the detection efficiencies determined by the two scaler biases was greatest for neutrons with energies 100 to 200 kev below the primary energy. Thus if considerable inelastic scattering occurred to a 150-kev level, the elastic cross section as determined from the low-bias scaler would be greater than that from the high-bias scaler, since some of the counts in the low-bias scaler would arise from inelastically scattered neutrons.

In Au and Pu^{239} , which have no levels in this region, one would expect no difference between the two biases and indeed none was observed. The level structure above 100 kev in U^{238} is not known, but the fact that the data from the two biases yield the same elastic cross section indicates no levels in the 100- to 200-kev region which contributes appreciably to inelastic scattering.

In U^{238} , however, a difference was observed between the two biases at both 0.5 Mev and 1.0 Mev, signifying inelastic scattering to one or more levels in the 150-kev region, and agreeing with data taken by other methods. The first excited state in U^{238} has been reported at 45 kev⁷⁻⁹ and recent inelastic scattering measurements¹⁰ indicate a second level at 150 kev. In addition, Batchelor¹¹ has found considerable inelastic scattering to low-lying levels in U^{238} .

In Figs. 3 and 4 the theoretical predictions¹² based on a complex square-well potential are given for U^{238} . These curves show the shape-elastic scattering only and do not include the elastic scattering following compound nucleus formation. The contribution of compound elastic scattering would add a component symmetric about 90°, but this is limited to the difference between the cross section for compound nucleus formation and the large cross section for inelastic collision. The parameters used were $V_0=42$ Mev, $R=1.45 \times 10^{-13} A^{1/3}$ cm, and $\zeta=0.03$ and 0.10. Table II lists the theoretical values of the total, elastic scattering, elastic transport, and compound nucleus formation cross sections. Although in general this potential, radius, and $\zeta=0.03$,² give a reasonable fit to the cross sections observed over most of the periodic table in this energy range, the agreement with the heavy-element angular distribution data is not good. However, it has been shown¹³ that a diffuse-edge nuclear potential with a smaller radius and greater depth gives better agreement between theory and experiment.

V. FISSION NEUTRON ANGULAR DISTRIBUTION

As stated in Sec. III, the counts in the third scaler were proportional to the number of fission neutrons. Since these data were taken at each angle, it was possible to obtain a relative angular distribution of fission neutrons produced by the primary energy neutrons. To do this, however, it was necessary to know the neutron spectrum at the sample in order to eliminate those fission neutrons produced by scattered neutrons, with the greatest source of these neutrons being the shield tank. This background correction was made as follows. The recoil counter was placed at the sample position and the number of counts per monitor count was observed with and without the shield tank in position. No difference was seen, indicating that the shield tank caused no significant increase in the flux of neutrons having an energy greater than 200 kev. The 200-kev lower limit was determined by the gamma-ray sensitiv-

⁷ N. P. Heydenburg and G. M. Temmer, Phys. Rev. **93**, 906 (1954).

⁸ Divatia, Davis, Moffat, and Lind, Phys. Rev. **100**, 1266 (1955).

⁹ R. B. Day (private communication).

¹⁰ R. C. Allen (private communication).

¹¹ R. Batchelor, Proc. Phys. Soc. (London) **A69**, 214 (1956).

¹² The authors are grateful to R. G. Thomas for providing these calculations.

¹³ J. R. Beyster and M. Walt (private communication).

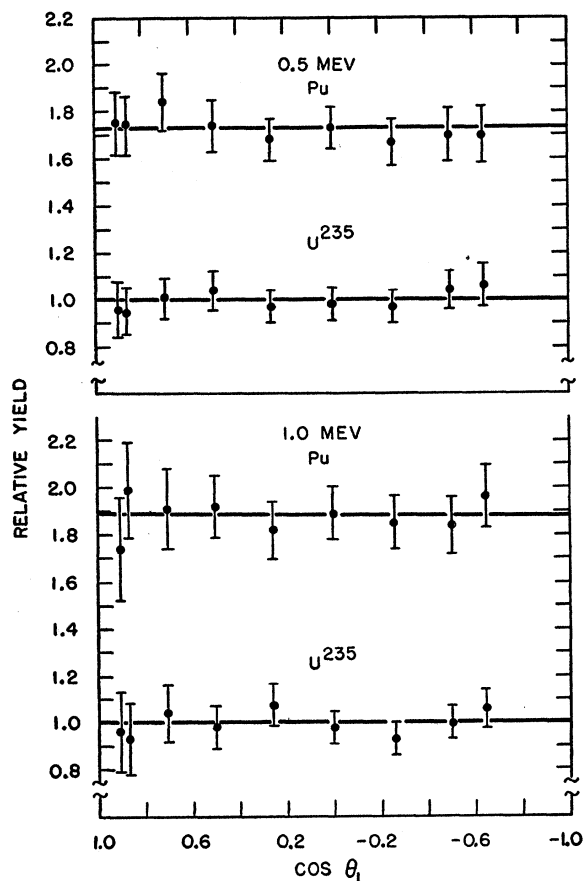


FIG. 5. The angular distributions of fission neutrons produced by 0.5-Mev and 1.0-Mev neutrons incident on U^{235} and Pu^{239} . The errors shown are the standard deviations of the relative yields and are due mostly to statistical errors at the small angles and to background corrections at the large angles.

ity of the counter. Next a U^{235} fission chamber was placed at the sample position. From the number of counts per monitor count with and without a cadmium shield and with and without the shield tank the spectrum at the sample position was determined. In the

worst case, with the shield tank at 130° , 95% of the neutrons were direct primaries, 3% of the neutrons had energies below 200 keV and above the cadmium resonance, and 2% were below the cadmium cut-off. At 0° , the middle group was negligible and the below-cadmium group was about 0.5%. To obtain the number of fission neutrons produced by these extra neutrons, thin shells of U^{235} were put around the fission chamber and the counting rate as a function of thickness was observed. From these data it was possible to deduce the thickness of the outer layer of the $\frac{3}{4}$ -inch-diameter scatterer affected by the slow neutrons and the magnitude of this effect relative to the fast-neutron effect. The correction to the actual fission angular distribution varied from 0% at 25° to 10% at 130° and was assumed to be the same for U^{235} and Pu^{239} .

The angular distributions of the fission neutrons are shown in Fig. 5. The U^{235} distributions are isotropic as expected since at these energies the neutrons are presumably emitted by the fragments which are known to be emitted isotropically.¹⁴ The neutrons emitted in Pu^{239} fission also have an isotropic distribution, indicating that the fragments are probably emitted isotropically. Since the number of fission neutrons detected was proportional to the product $\sigma_f \bar{\nu}$, where σ_f is the fission cross section and $\bar{\nu}$ is the average number of neutrons emitted per fission, the ratio of these products for the two elements was obtained at each energy. Using the known fission cross sections it was found that $\bar{\nu}(Pu^{239})/\bar{\nu}(U^{235}) = 1.3 \pm 0.2$ at both energies, agreeing with the empirical theory¹⁵ based on the boil-off of neutrons from excited fission fragments.

ACKNOWLEDGMENTS

The authors are very grateful to Dr. Martin Walt for many helpful discussions, particularly those relating to the multiple scattering corrections. To Chester Kazek, Jr., we owe our thanks in connection with the IBM 701 calculations.

¹⁴ Brolley, Dickinson, and Henkel, *Phys. Rev.* **99**, 159 (1955).

¹⁵ R. B. Leachman, *Phys. Rev.* **101**, 1005 (1956).